Recruitment of dynein to late endosomes and lysosomes through light intermediate chains

Serena C. Tan, Julian Scherer, and Richard B. Vallee
Department of Pathology, College of Physicians and Surgeons, Columbia University, New York, NY 10032

ABSTRACT Cytoplasmic dynein is involved in a wide range of cellular processes, but how it is regulated and how it recognizes an extremely wide range of cargo are incompletely understood. The dynein light intermediate chains, LIC1 and LIC2 (DYNC1LI1 and DYNC1LI2, respectively), have been implicated in cargo binding, but their full range of functions is unknown. Using LIC isoform-specific antibodies, we report the first characterization of their subcellular distribution and identify a specific association with elements of the late endocytic pathway, but not other vesicular compartments. LIC1 and LIC2 RNA interference (RNAi) each specifically disrupts the distribution of lysosomes and late endosomes. Stimulation of dynein-mediated late-endosomal transport by the Rab7-interacting lysosomal protein (RILP) is reversed by LIC1 RNAi, which displaces dynein, but not dynactin, from these structures. Conversely, expression of ΔN-RILP or the dynactin subunit dynamitin each fails to displace dynein, but not dynactin. Thus, using a variety of complementary approaches, our results indicate a novel specific role for the LICs in dynein recruitment to components of the late endocytic pathway.

INTRODUCTION

Cytoplasmic dynein is a multisubunit motor protein that produces force toward the minus ends of microtubules. In addition to roles in mitosis and cell migration (Dujardin et al., 2003), it is also responsible for several forms of vesicular transport, including the maintenance and regulation of late endocytic transport (Burkhardt et al., 1997; Deacon et al., 2003; Bananis et al., 2004). The mechanisms by which dynein is recruited to vesicular organelles and how its function is regulated at these sites, however, are only partially understood.

Cytoplasmic dynein consists of two heavy chains (HCs), each of which contains a motor domain, and multiple accessory subunits, including intermediate chains (ICs), light chains (LCs), and light intermediate chains (LICs). The accessory subunits have been implicated in dynein cargo binding, in some cases through complex mechanisms. The ICs interact with the multisubunit dynein accessory protein complex, dynactin, through its p150[Glued] subunit (Karki and Holzbaur, 1995; Vaughan and Vallee, 1995). Dynactin, in turn, has been implicated in dynein cargo attachment to multiple structures, including mitotic kinetochores (Echeverri et al., 1996) and the Golgi apparatus (Roghi and Allan, 1999). The ICs have also been found to interact directly with potential cargo proteins (Karki et al., 2002; Caviston et al., 2007). The dynein LCs LC8 (DYNLL), Tctex1 and RP3 (DYNLT), and Rbl (DYNLRB) associate with the ICs. Although the LCs interact with diverse protein partners (Tai et al., 1999; Tai et al., 2001; Yeh et al., 2006; Lo et al., 2007), many of these interactions are now thought to be independent of their association with the dynein complex (Williams et al., 2007).

The LICs represent an additional class of dynein accessory subunits LIC1, LIC2, and LIC3 (DYNC1LI1, DYNC1LI2, and DYNC2LI3), which are encoded by three genes. LIC1 and LIC2 are 65% identical and associate with the major form of cytoplasmic dynein, dynein 1 (Tynan et al., 2000a). LIC3 (also known as D2LIC) is highly divergent from the other LICs and is the only known accessory subunit of a second form of cytoplasmic dynein, dynein 2, which functions only

Abbreviations used: BSA, bovine serum albumin; DAPI, 4′,6-diamino-2-phenylindole; EEA1, early endosome antigen 1; EGFR, epidermal growth factor receptor; ESCRT-II, endosomal sorting complex required for transport II; HC, heavy chain; IC, intermediate chain; LAMP1, lysosomal-associated membrane protein 1; LC, light chain; LIC1, dynein light intermediate chain 1; LIC2, dynein light intermediate chain 2; PBS, phosphate-buffered saline; PNS, postnuclear supernatant; RILP, Rab7-interacting lysosomal protein; RNAi, RNA interference; siRNA, small interfering RNA.
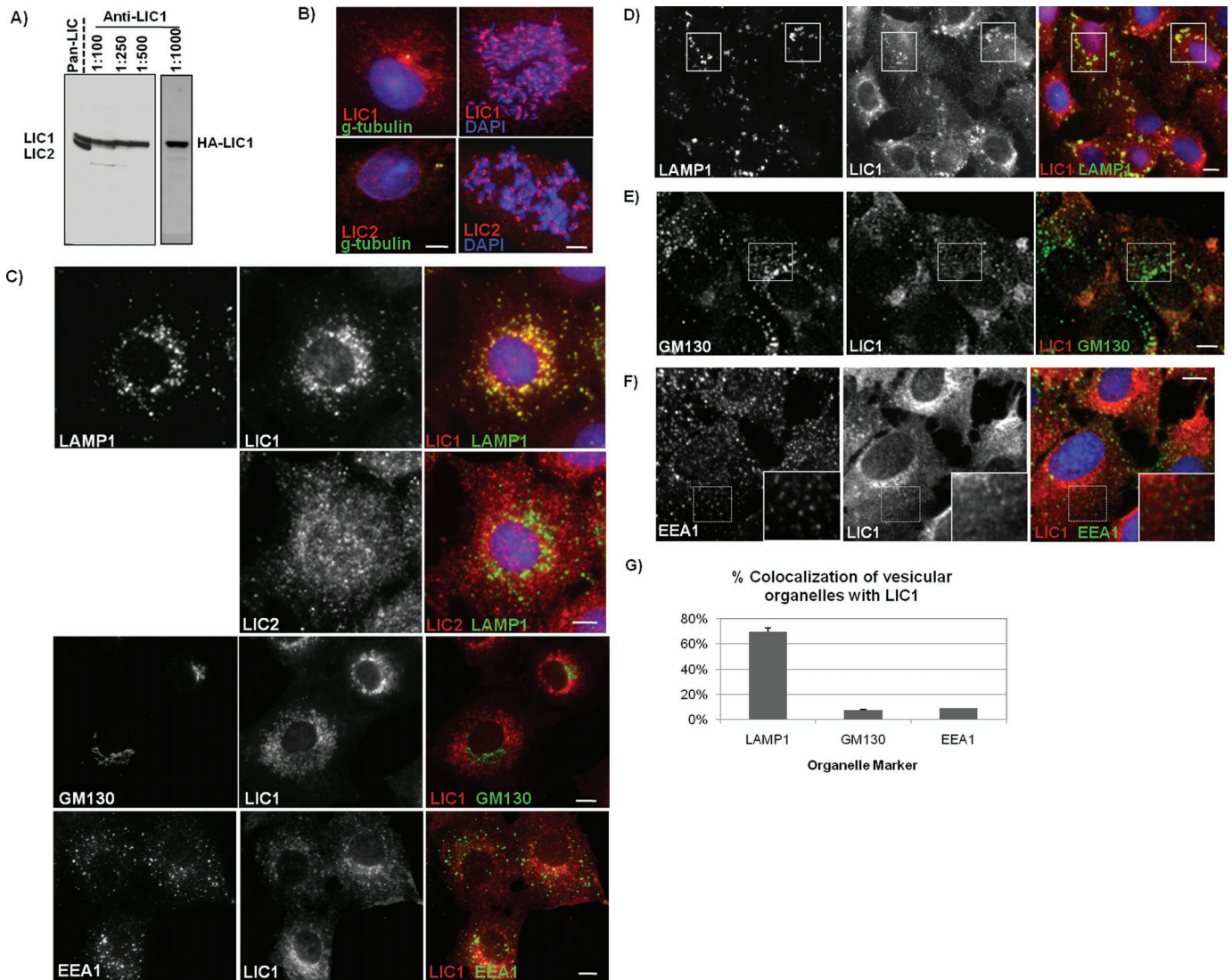
FIGURE 1: LICs localize to common and distinct subcellular structures and are absent from the Golgi and early endosomes. (A) Comparison of chicken anti-LIC1 with the rabbit pan-LIC antibody via SDS–PAGE and Western blotting on lysates from Rat2 fibroblasts. The pan-LIC antibody recognizes both LIC1 and LIC2 while anti-LIC1 specifically recognizes both endogenous LIC1 and overexpressed HA-LIC1 (right panel). (B) Immunocytochemistry of LIC1 and LIC2. Rat2 cells are triple labeled (left) for DNA (blue, DAPI), centrosomes (green, γ-tubulin), and LIC1 or LIC2 (red, anti-LIC1, anti-LIC2) or double labeled (right) for DNA (blue) and LIC1 or LIC2 (red). (C–F) Immunocytochemistry of cells costained with antibodies to LIC1 and/or LIC2 (LICs are shown in red in merged images) and the respective organelle markers, LAMP1 (C, D), GM130 (C, E), or EEA1 (C, F) (shown in green). (C) LIC1 shows clear colocalization with LAMP1-positive lysosomes both peripherally and in the perinuclear space while LIC2 staining is more diffuse and shows little colocalization with LAMP1 staining. Furthermore, little to no colocalization is seen for LIC1 with GM130 or EEA1 staining. (D–F) Cells were treated with 10 μM nocodazole to depolymerize microtubules and disperse lysosomes (D), Golgi elements (E), and early endosomes (F) and then stained for LIC1 and the respective organelle markers. Boxes highlight clear LIC1 colocalization with dispersed LAMP1-positive lysosomes (D). Minimal colocalization is seen between dispersed Golgi elements and LIC1 (E). Early endosomes labeled with EEA1 show no colocalization with LIC1 (F). Insets are zoomed images of areas outlined in hashed boxes. (G) Quantification of the percentage of LAMP1-, GM130-, or EEA1-positive structures colocalizing with LIC1 staining. For each organelle marker, the number of LAMP1-, GM130-, or EEA1-positive structures colocalizing with LIC1 puncta was counted in 30 cells and represented as percent colocalization with LIC1. Scale bars, 5 μm.

in intraflagellar transport (Grissom *et al.*, 2002; Mikami *et al.*, 2002; Perrone *et al.*, 2003). While LIC1 and LIC2 self-associate, heterologous LIC interactions have not been observed, and cytoplasmic dynein appears to exist in separate LIC1- and LIC2-containing pools (Tynan *et al.*, 2000a). LIC1, but not LIC2, interacts with pericentrin and has been proposed to participate in its recruitment to centrosomes (Purohit *et al.*, 1999; Tynan *et al.*, 2000b). LIC2, but not

LIC1, has been found to interact with Par3 and serve a role in regulating microtubule dynamics and centrosome polarization in migrating cells (Schmoranzer *et al.*, 2009). The subcellular distribution of LIC1 and LIC2 has not been investigated. In *Caenorhabditis elegans*, which contains instead of LIC1 and LIC2 a single dynein 1 LIC, *DLI-1*, mutational analysis has identified diverse defects in mitosis, including defective centrosome separation (Yoder and Han,
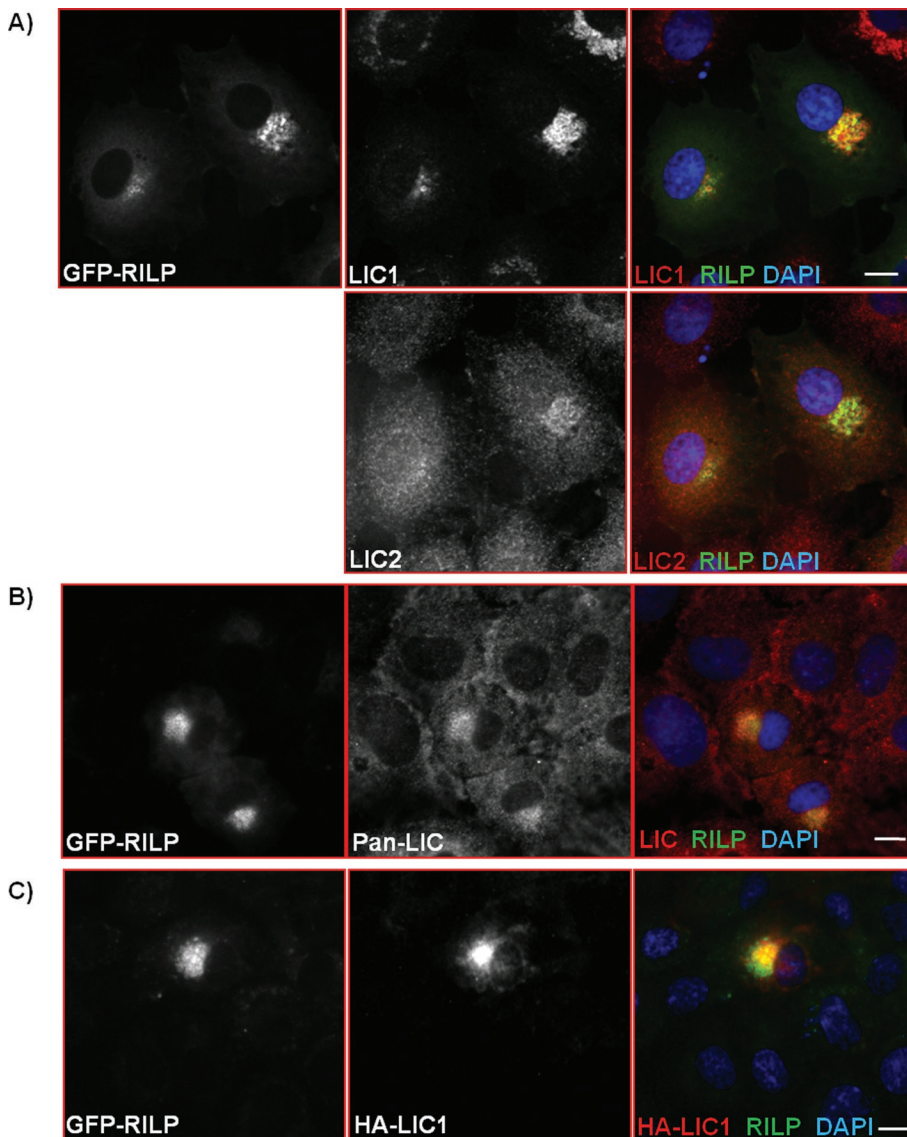
FIGURE 2: Dynein is enriched on RILP clustered lysosomes. Immunocytochemistry of LIC1 and LIC2 (A), both LICs together as detected with pan-LIC antibody (B), and overexpressed HA-LIC1 (C) in Rat2 cells overexpressing GFP-RILP. Scale bars, 5 µm.

recruitment of dynactin. These results identify through a variety of approaches a dynein recruitment mechanism distinct from that described for other organelles, revealing unexpected diversity in the regulation of motor protein–cargo interactions and organelle maintenance.

RESULTS

Subcellular localization of LICs

To determine the relative cellular distributions of LIC1 and LIC2, we prepared a chicken antibody to a unique C-terminal LIC1 peptide to complement the rabbit anti-LIC2 and pan-LIC antibodies we previously produced (Tynan *et al.*, 2000b). Analysis of lysates from Rat2 fibroblasts by SDS–PAGE and Western blotting (Figure 1A) revealed that the anti-LIC1 antibody showed exclusive reactivity with endogenous LIC1 while the pan-LIC antibody recognized both LIC1 and LIC2 simultaneously, as shown previously (Tynan *et al.*, 2000b).

Immunofluorescence microscopy with our LIC-specific antibodies showed both LIC1 and LIC2 to localize to centrosomes in interphase cells and kinetochores in mitotic cells (Figure 1B). In addition, extensive diffuse and punctate staining was detected in the cytoplasm of interphase cells by each antibody. Intriguingly, LIC1 exhibited discrete, bright colocalization with lysosomal-associated membrane protein 1 (LAMP1)–positive lysosomes/late endosomes, which, however, was not readily detected using anti-LIC2 (Figure 1C, top). LIC1 also strongly colocalized with another lysosome/late endosome marker, GFP-CD63 (Supplemental Figure S1). Little to no colocalization, however, was seen for either LIC with the Golgi marker GM130 or the early endosome antigen 1 (EEA1) marker (Figure 1C, middle and bottom). Nocodazole was used to redistribute membranous organelles and to test for localization to discrete vesicular structures. LIC1 redistributed with LAMP1-positive structures under these conditions (Figure 1D), whereas LIC2 localization was still largely undetectable (unpublished data). Individual GM130-positive puncta generated by nocodazole treatment were mostly negative for LIC1 (Figure 1E), and little LIC1 colocalization was detected with the marker EEA1 (Figure 1F) or green fluorescent protein (GFP)–Rab5 (unpublished data). A comparison of colocalization of LIC1 staining with these various membrane markers shows a unique colocalization with late endocytic membranes (Figure 1G).

As an additional test for colocalization of dynein subunits with late endocytic structures, we expressed the RILP. Consistent with earlier reports (Jordens *et al.*, 2001), RILP overexpression resulted in tightly packed perinuclear clusters of late endosomes and lysosomes with enhanced reactivity to antibodies against cytoplasmic dynein. We found LIC1 immunoreactivity to be strongly concentrated in these clusters (Figure 2A). In this case LIC2 staining

2001). *DLI-1* was also found to bind to the centrosome–nucleus linker protein ZYG-12 (Malone *et al.*, 2003). *C. elegans DLI-1* mutants also display abnormal accumulations of the synaptic protein synaptobrevin at ends of neuronal processes (Koushika *et al.*, 2004), suggesting a role in retrograde axonal transport. Injection of an antibody to the LICs in *Xenopus* melanophores also interfered with movement of melanosomes toward the cell center (Reilein *et al.*, 2003). Taken together, these results suggest a broad range of function for the LICs but provide limited insight into specific sites of action and relative functions of the higher eukaryotic LICs, LIC1 and LIC2.

This study was initiated to define and compare the cellular distribution and functions of LIC1 and LIC2. We find each LIC to localize to kinetochores and centrosomes, known dynein functional sites, but to participate in a limited and specific aspect of vesicular dynein function, especially in the late endocytic pathway. We present evidence that LIC1 is required for dynein recruitment to lysosomes and late endosomes, independent of the previously reported Rab7-interacting lysosomal protein (RILP)–dependent
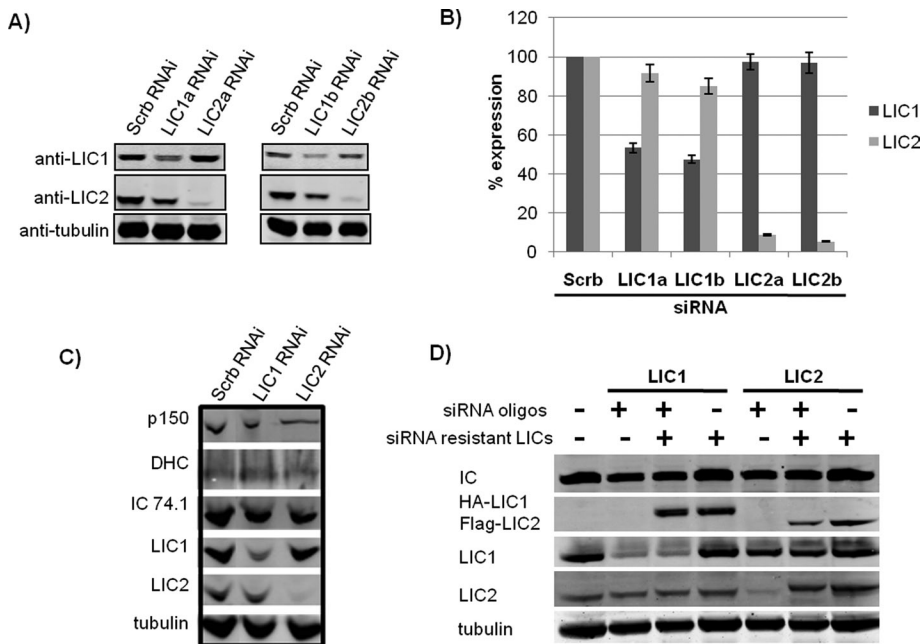
FIGURE 3: RNAi against LIC1 and LIC2 specifically knocks down endogenous LICs without affecting levels of siRNA-resistant LICs or other dynein and dynactin proteins. (A) Western blots of Rat2 cell lysates after 48 h treatment with scrambled siRNA or siRNA against LIC1 or LIC2 specifically and blotted with antibodies to LIC1, LIC2, and α-tubulin as a loading control. (B) Quantification of knockdown for LIC1 and LIC2 RNAi. LIC1 and LIC2 protein levels are shown as percentages of LIC1 and LIC2 levels in scrambled control RNAi conditions. Values shown are averages from immunoblotting of three independent RNAi experiments. Quantitation of immunoreactive intensities was performed and analyzed using ImageJ. (C) Immunoblotting of dynein IC, HC, LIC1, LIC2, and the dynactin subunit p150^{Glued} of Rat2 cell lysates after 48 h treatment with scrambled siRNA or siRNA against LIC1 or LIC2 specifically, with α-tubulin as a loading control. (D) Western blot of Rat2 cell lysates after transfection with siRNA (72 h) and siRNA-resistant constructs (48 h) and blotted with antibodies to dynein IC, LIC1, LIC2, HA-tag, Flag-tag, and α-tubulin as a loading control. Note that the signal for HA-LIC1 does not interfere with the endogenous LIC1 signal in contrast to the signal for Flag-LIC2, which interferes with the endogenous LIC2 signal.

colocalized with RILP, but at lower intensity than for LIC1 (Figure 2A). Staining of the RILP-clustered vesicles could also be detected with a pan-LIC antibody (Figure 2B), as could heterologously expressed HA-LIC1 (Figure 2C).

LIC RNAi interference (RNAi) effects on membrane behavior
To test for a physiological role for the LICs in control of vesicular behavior, we transfected Rat2 fibroblasts with LIC1- and LIC2-specific small interfering RNAs (siRNAs), each of which clearly and specifically reduced LIC protein levels (Figure 3, A and B; Supplemental Figure S2, A and B) without affecting the opposite LIC or other dynein and dynactin subunits (Figure 3C). The LIC1 and LIC2 siRNAs also specifically knocked down the recombinant wild-type HA-LIC1 and Flag-LIC2 (Supplemental Figure S2C). RNAi-resistant HA-LIC1 and Flag-LIC2 levels were not affected by the siRNAs (Figure 3D), and the expressed polypeptides were found to incorporate into the dynein complex (Supplemental Figure S2D). We also saw little to no effect of LIC RNAi on the integrity of the dynein complex as assayed by sucrose density centrifugation (Supplemental Figure S3).

After 3 d of knockdown of LIC1 or LIC2 alone (Figure 4A), LAMP1-positive vesicles, which are normally concentrated around the centrosome, were distributed more broadly. Equally striking, these structures were brighter, and many were also considerably enlarged. Quantification of the percent area of LAMP1 fluorescence within

individual cells shows that knockdown of LIC1, LIC2 (Figure 4C), or both LIC1 and LIC2 together (unpublished data) resulted in up to a threefold increase in area of LAMP1 fluorescence compared with control cells. Comparable effects of LIC RNAi were also seen for lysosomes labeled with the live-cell lysosomal marker LysoTracker-Red (Supplemental Figure S4). The increase in cell area occupied by lysosomes was rescued to the control value by the RNAi-resistant LIC1. However, the enhancement of the lysosome signal was only partially reversed. In stark contrast to LIC1, LIC2 overexpression itself caused a pronounced lysosome phenotype similar to that produced by RNAi, and rescue experiments were therefore not possible for LIC2 (Figure 4, B and C).

To test for defects in the distribution of other organelles, we stained cells subjected to LIC RNAi with markers for the Golgi apparatus and early endosomes. Despite the noticeable changes observed in late endosomes and lysosomes, we saw no detectable effect of LIC knockdown on Golgi organization, even with double LIC knockdown (Figure 4D), or on the distribution of EEA1-positive early endosomes (Figure 4E) relative to control cells. Together, these results were consistent with the limited subcellular distribution we observed for the LICs. We also monitored epidermal growth factor receptor (EGFR) degradation to test for effects of LIC RNAi on endocytic trafficking. Immunostaining intensity for EGFR was markedly reduced by 30 min in control cells but persisted after treating cells with siRNAs against LIC1 (Figure 5) and LIC2 (unpublished data). Similar results were also observed in cells overexpressing recombinant GFP-EGFR when treated with siRNAs against the LICs (unpublished data).

We also tested for dynein cofractionation with late endocytic vesicles using a sucrose density gradient membrane flotation protocol (Aniento et al., 1993) (Figure 6A). Dynein ICs and both LICs were present in the lightest endosomal fraction (27–8% sucrose boundary), which is highly enriched for LAMP1-positive late endosomal structures (Aniento et al., 1993) and which we also find to be depleted in EEA1-positive early endosomes. The dynein subunits were also detected in the heavier endosomal fraction (35–27% sucrose boundary), which contained a mixture of LAMP1- and EEA1-positive endosomes, and in fractions from the 40–35% sucrose boundary, which contained mixed populations of heavy unfractionated membranes. Dynein subunits also cofractionated with expressed GFP-RILP as an additional late endocytic marker (Figure 6B). RILP expression caused a relative shift in the distribution of the dynein markers to the lighter endocytic fractions, providing direct biochemical evidence for RILP recruitment of dynein to this specific organelle class. RNAi knockdown of the LICs displaced dynein from the light endocytic fractions (Figure 6, C and D). The effect of LIC1 RNAi was particularly severe (Figure 6C). In each case, however, we noted a substantial increase in the intensity of LAMP1 immunoreactivity as well as a shift to higher densities, a likely correlate of the enhanced
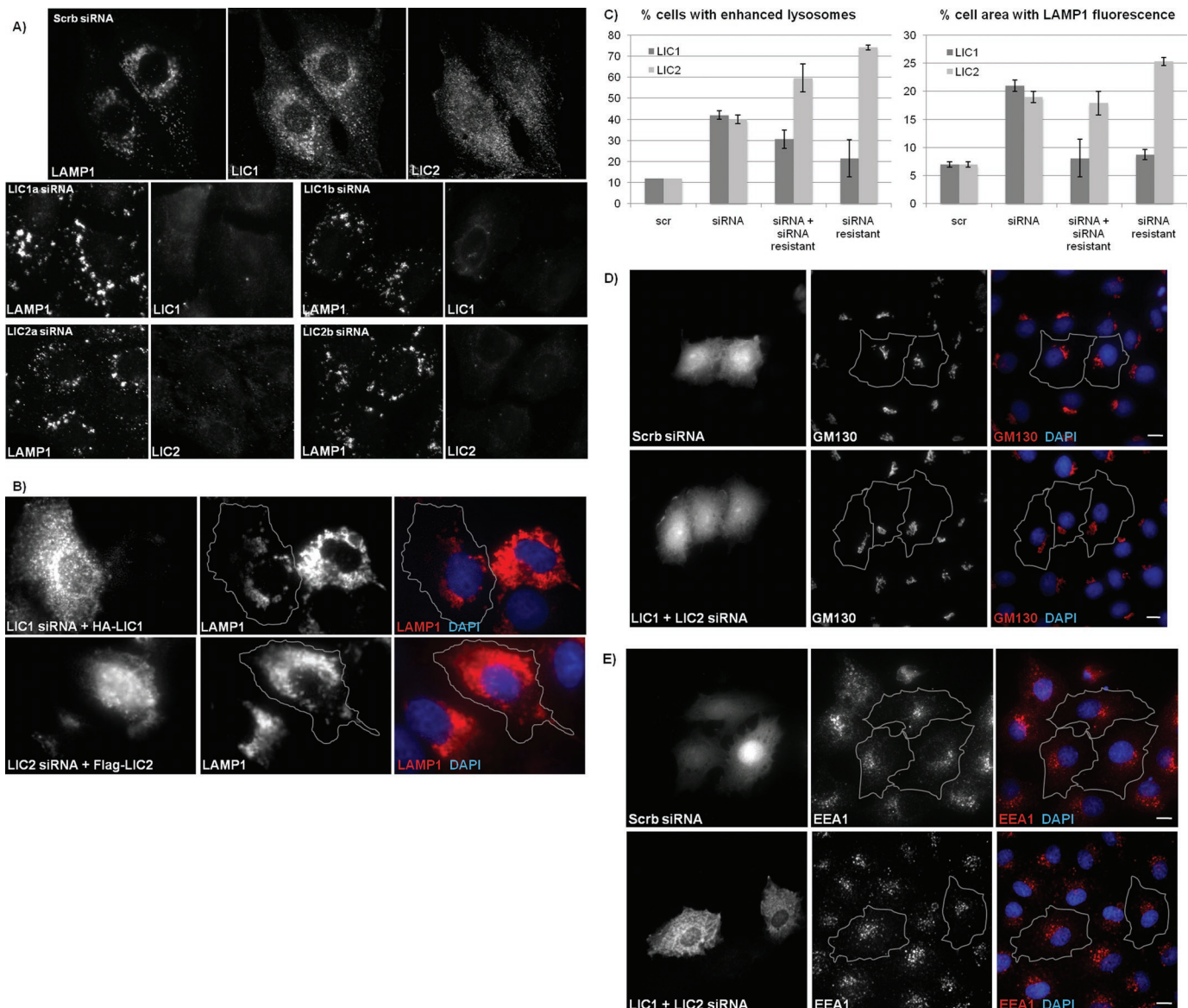
FIGURE 4: RNAi of LIC1 and LIC2 causes enlarged and brighter lysosomes and disrupts lysosomal distribution but has no effect on early endosomes or the Golgi. (A) Rat2 cells were treated with scrambled, LIC1, or LIC2 RNAi and then costained for LAMP1 and LIC1 or LIC2. (B) Rat2 cells transfected with LIC siRNA and siRNA-resistant HA-LIC1 or Flag-LIC2 rescue constructs and costained for LAMP1, HA, or Flag and for DNA with DAPI. Gray lines delineate individual cell boundaries of siRNA-resistant LIC-overexpressing cells. (C) Quantification of the percentage of cells displaying altered late endosome/lysosome phenotype (left graph) and for the percent cell area of LAMP1 fluorescence per cell (right graph). The total area of positive LAMP1 staining within a cell is shown as a percentage of total cell area. Averages are shown where at least 30 cells were counted per condition from each of three experiments. (D, E) Rat2 cells were cotransfected with GFP and either scrambled RNAi or both LIC1 and LIC2 RNAi together and stained for Golgi with anti-GM130 (D) or early endosomes with anti-EEA1 (E) in red and for DNA with DAPI in blue. Gray lines delineate individual cell boundaries of transfected cells. Scale bars, 5 μm.

lysosome size and LAMP1 immunoreactivity we observed in LIC-depleted cells (discussed previously). We note that evidence for similar cytochemical and biochemical enhancement of lysosomes and lysosomal markers has been reported to result from RILP RNAi (Progida *et al.*, 2007).

Role of LICs versus dynactin in lysosomal dynein recruitment
To test the contributions of the LICs to RILP-mediated late endo-somal clustering, we cotransfected cells with GFP-RILP and LIC siRNAs. LIC1 RNAi caused a partial dispersal of the RILP-positive clusters as well as enlargement of individual RILP-positive vesicles

(Figure 7). The percentage of area occupied by RILP-associated structures within individual cells is quantified in Figure 8E. Knock-down of LIC1 resulted in up to a fourfold increase in the percentage of cell area occupied by the RILP clusters compared with control. Upon further inspection, we observed that in 68% of these cells, LIC1 RNAi resulted in a significant loss of dynein IC immunoreactiv-ity and colocalization with the RILP-positive vesicular structures (Figure 7B), whereas the dynactin polypeptide p150[Glued] was still clearly present and enriched on these vesicles (Figure 7C). These findings suggest that LIC1 may have a role in recruitment of dynein to lysosomes independent of dynactin. In contrast to these results,
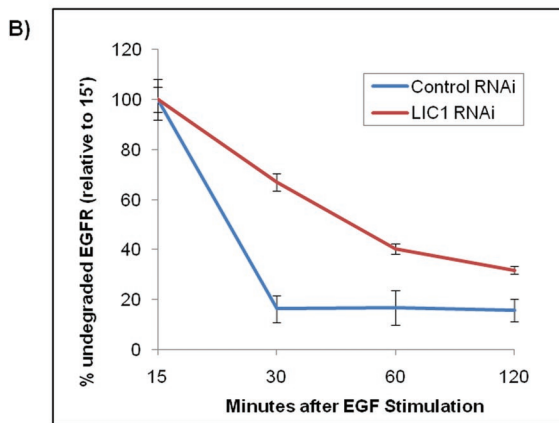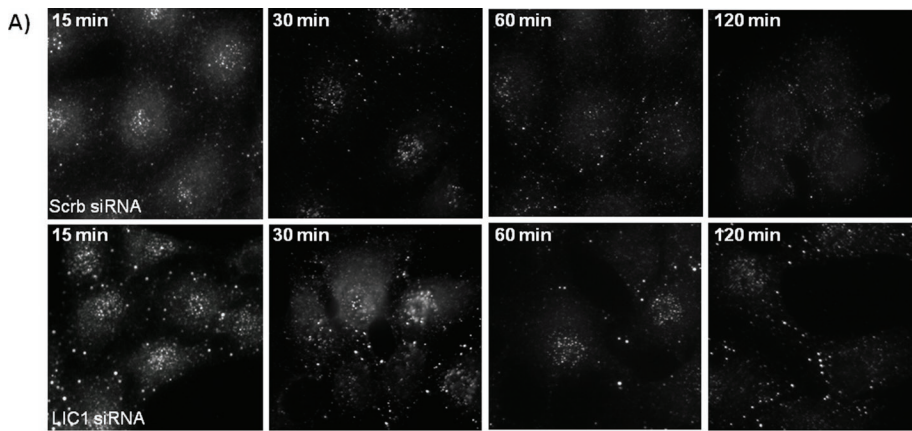
FIGURE 5: LIC1 RNAi causes a temporal delay in the degradation of EGF receptor (EGFR). (A) Rat2 cells treated with scrambled RNAi or RNAi against LIC1 were pretreated with 10 µg/ml cycloheximide before being stimulated for 15, 60, 120, or 180 min with 50 ng/ml EGF and stained for EGFR. (B) The intensities of the EGFR staining were quantified and plotted as a percentage of the respective intensities after 15 min EGF stimulation.

knockdown of LIC2 had little effect on the ability of RILP to cluster lysosomes in the centrosomal region (Figure 8E). In this case, we also found dynein to remain localized to the intact RILP clusters (unpublished data).

These results suggest that the LICs, particularly LIC1, might be involved in dynein recruitment to late endosomal structures independently of dynactin. To test this hypothesis, we expressed a GFP-tagged C-terminal RILP fragment (ΔN-RILP), which lacks the dynactin interaction domain. Although this fragment is still capable of binding to lysosomes through Rab7, dynactin is lost from lysosomes, which disperse throughout the cytoplasm (Jordens et al., 2001; Wu et al., 2005). We observed that, despite the clear dispersal of lysosomes by N-RILP, they remained highly immunoreactive for LIC1 (Figure 8A).

To address this issue further, we disrupted the dynein–dynactin complex by overexpressing the dynamitin subunit of dynactin (Figure 8, B–D), which interferes with the interaction between dynein and dynactin (Echeverri et al., 1996). Coexpression of myc-dynamitin with GFP-RILP caused partial dissociation of the RILP cluster and enlargement of individual vesicles (Figure 8, B–E), consistent with our observations for LIC1 RNAi (Figure 7). However, despite the loss of p150^{Glued} from these structures (Figure 8B), both dynein HC and LIC1 remained associated with them (Figure 8, C and D). We obtained similar results using another late endosome and lysosome marker, GFP-Rab7, coexpressed with myc-dynamitin

(Supplemental Figure S5A). Again, the GFP–Rab7-positive lysosomes were dispersed, but LIC1 was still retained. LIC1 also remained localized to LAMP1-positive lysosomes after overexpression of myc-dynamitin alone (Supplemental Figure S5B). These findings indicate that dynein may indeed be localized to lysosomes independently of dynactin.

We previously reported an involvement of the kinetochore protein ZW10 in dynein-mediated vesicular transport (Varma et al., 2006). We note dispersal of lysosomes by ZW10 RNAi in control cells, as expected from that study (unpublished data). However, ZW10 RNAi had no effect on RILP-mediated clustering of lysosomes or dynein or dynactin localization to these structures (Supplemental Figure S6A), nor was ZW10 observed to accumulate at these sites (Supplemental Figure S6B).

DISCUSSION
Dynein LICs are among the least studied subunits of the dynein complex. We find that they localize to well-established sites for dynein function—kinetochores and centrosomes—but have an unexpectedly selective interaction with vesicular structures in the late endosome/lysosome pathway. LIC1 is more clearly associated with these structures than LIC2, though RNAi for either isoform affects late endosome/lysosome distribution and morphology. In marked contrast to mechanisms used by other physiological dynein cargo, these structures have no clear requirement for dynactin in dynein recruitment, a function that appears, instead, to be under the direct control of the LICs.

Organelle-specific LIC distribution and function
Using LIC-specific antibodies, we have obtained the first localization data for LIC1 and LIC2. We find both to be associated with mitotic kinetochores and centrosomes/spindle poles, suggesting at least some degree of functional redundancy. This distribution is also consistent with roles for the LICs in mitosis (Dell et al., 2000; Yoder and Han, 2001), centrosome assembly (Purohit et al., 1999; Young et al., 2000), and linkage of the centrosome to the nucleus (Yoder and Han, 2001; Malone et al., 2003). The detailed roles of the LICs at mitotic structures remain to be explored more fully. LIC1 showed clear localization to late endosomes/lysosomes, and RNAi for each LIC disrupted these structures. The limited anti-LIC2 staining could reflect an antibody accessibility problem, though the same antibody clearly recognizes LIC2 at kinetochores and centrosomes. It seems more reasonable, therefore, that LIC1 and LIC2 have overlapping functions but that LIC1 plays a more critical role in the endocytic pathway in the cell types used in this study.

In contrast, both LICs were largely absent from early endosomes and the Golgi apparatus, and knockdown of the LICs had no effect on the distribution of these structures. This is despite
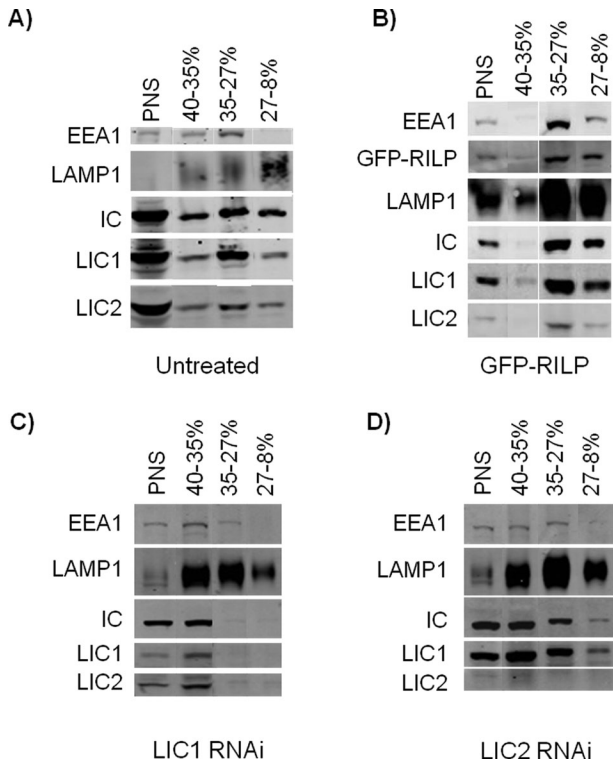
FIGURE 6: Cofractionation of dynein with late endosomes and lysosomes in sucrose density gradient membrane flotation assays. (A) Dynein IC, LIC 1, and LIC 2 all cofractionate with LAMP1-positive structures in sucrose density gradient membrane flotation assays. EEA1-positive early endosomes were found at both the 40–35% and the 35–27% sucrose interfaces while a fraction enriched for LAMP1-positive vesicles and de-enriched for EEA1-positive vesicles is found at the upper interface of 27–8% sucrose and is positive for dynein IC, LIC1, and LIC2. The starting homogenate of postnuclear supernatant (PNS) is shown in the first lane. (B) Dynein IC, LIC1, and LIC2 cofractionate with overexpressed GFP-RILP and are further enriched in the light late endocytic fraction at the interface of 27–8% sucrose. (C) Dynein IC is displaced from the lighter fractions of purified lysosomes and late endosomes (35–27% and 27–8% sucrose boundaries) after 48 h RNAi treatment against LIC1. (D) Dynein IC is also displaced from this fraction by LIC2 RNAi, although to a lesser extent. In both RNAi conditions, an overall increase is seen in the levels of LAMP1 (C, D).

well-established evidence for a role for cytoplasmic dynein in controlling Golgi distribution (Presley *et al.*, 1997; Burkhardt, 1998; Harada *et al.*, 1998; Lippincott-Schwartz, 1998) and more recent evidence for a role in microtubule minus end–directed transport of early endosomes (Habermann *et al.*, 2001; Driskell *et al.*, 2007). Recruitment of cytoplasmic dynein to these structures involves factors both unique and common to multiple membrane compartments (Holleran *et al.*, 2001; Matanis *et al.*, 2002; Short *et al.*, 2002), as may be the case for dynein subunits (this study; Ha *et al.*, 2008). The lack of effect of RNAi for LIC1, LIC2, or both on Golgi or early endosome organization argues against a physiological role for the LICs at these structures. We note that an effect on the Golgi apparatus has been reported in one study (Palmer *et al.*, 2009) but disputed in another (Sivaram *et al.*, 2009). The combination of localization and phenotypic analysis argues strongly against such a role, at least in the cells used in our study.

Nature of endosome/lysosome defect

LIC1 RNAi causes redistribution of LAMP1- and LysoTracker-positive membranes, but equally striking are the enlargement of these structures, an increase in immunofluorescence intensity for lysosomal markers, and the disruption of endocytic transport as seen by inhibition of EGFR degradation. Although these effects have not been previously described for dynein-inhibited cells, they are strongly consistent with the effects of RILP RNAi (Progida *et al.*, 2007), which resulted in elevated levels of LAMP1 and other late endosomal markers, enlargement and increased immunoreactivity of late endocytic structures, and inhibition of EGFR degradation. RILP interacts not only with dynactin (Jordens *et al.*, 2001) but also with the endosomal sorting complex required for transport II (ESCRT-II), which mediates endosome sorting and biogenesis (Progida *et al.*, 2006; Wang and Hong, 2006). Conceivably, therefore, the effects of LIC inhibition could somehow reflect defects in ESCRT-II–mediated membrane trafficking. Alternatively, the phenotype may well result from altered dynein function. In support of this possibility, dynamitin overexpression produced effects on late endosome/lysosome morphology very similar to those seen with RILP RNAi. Furthermore, the same phenotype is produced by expression of the ΔN-RILP fragment (Figure 8A), which acts by displacement of dynactin from lysosomes. How reduction in dynein/dynactin activity may contribute to the formation of enlarged endosomal/lysosomal structures is uncertain. The enlarged structures are positive for LAMP1, LysoTracker, RILP, dynein, dynactin, and Rab7 and devoid of Rab5 and EEA1. These observations suggest that formation of late endosomes and lysosomes persists in LIC-, RILP-, and dynactin-inhibited cells; perhaps it is exit or recycling from this compartment that is defective.

Contribution of LIC1 to late endocytic dynein recruitment

Our evidence supports a role for LIC1 in particular in dynein recruitment to late endosomes and lysosomes (summarized in Figure 9A). Knockdown of LIC1 displaced dynein from RILP-induced clusters. Conversely, neither expression of ΔN-RILP nor the dynamitin subunit of dynactin had an effect on dynein localization to lysosomes. Of considerable interest, expression of ΔN-RILP clearly displaced p150[Glued] from lysosomes and late endosomes, but LIC1 remained. LIC1 binding was also unaffected by dynamitin overexpression, which disrupts dynactin structure and is known to displace dynein from kinetochores and from the Golgi apparatus. Coexpression of RILP with dynamitin resulted in enlarged RILP-containing vesicles that lacked dynactin but retained LIC1 and dynein HC. Taken together, these results indicate that while both dynein and dynactin are needed for maintenance of normal endosomal and lysosomal distribution, the two protein complexes are recruited to these vesicles separately and independently (Figure 9B).

Nonetheless, because inhibition of either dynactin or dynein disrupts normal late endosome and lysosome behavior, each complex is clearly required for proper organelle behavior. Whether dynein and dynactin require their established IC-p150[Glued] linkage to perform this function, or only under circumstances when dynactin acts to recruit dynein, is unknown. Dynactin has been found to increase the processivity of dynein-mediated movement along microtubules (King and Schroer, 2000; Haghnia *et al.*, 2007). This effect was observed using individual complexes bound to latex beads as a mixture, suggesting that a direct, physiological link is not required.

Finally, our results suggest that at least one other factor implicated in endosome and lysosome dynein function, ZW10 (Varma *et al.*, 2006), acts independently of RILP. Conceivably, these results
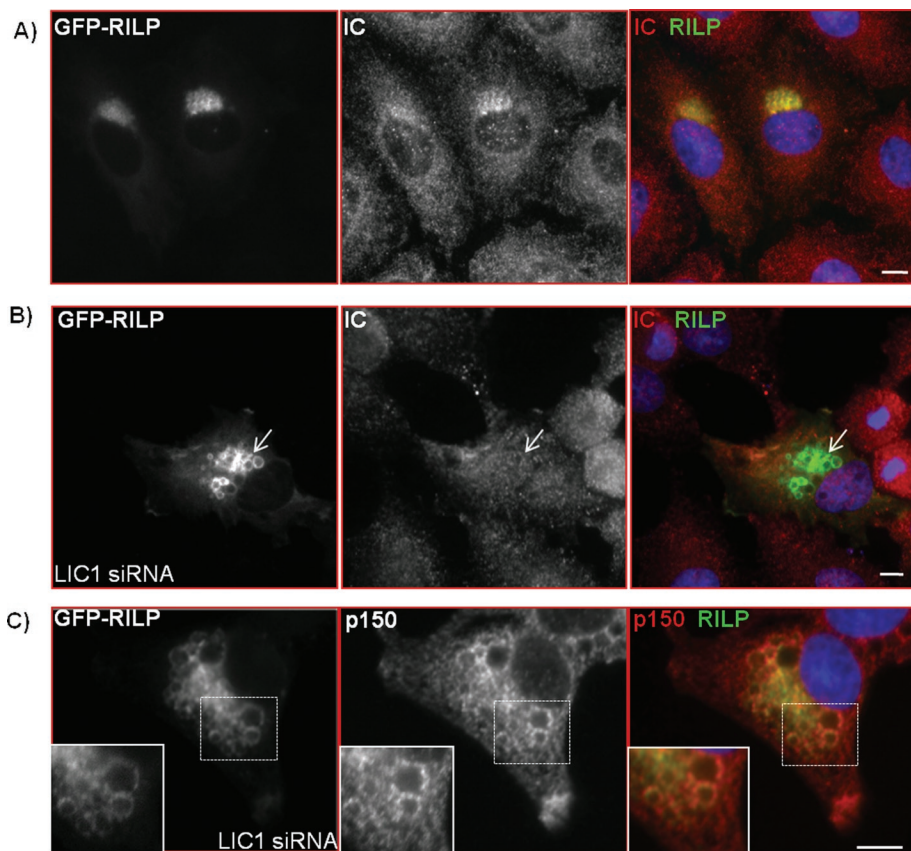
FIGURE 7: Knockdown of LIC1 disrupts RILP clusters and vesicles and displaces dynein independently of dynactin. Immunocytochemistry of dynein IC (red) in cells overexpressing GFP-RILP alone (A) or cotransfected with LIC1 RNAi (B). Arrows indicate the loss of IC staining from RILP vesicles in cells treated with LIC1 siRNA. (C) Immunostaining of the dynactin subunit p150[Glued] (red) in cells treated with LIC1 RNAi and overexpressing GFP-RILP. Distinct p150[Glued] puncta remain localized to enlarged RILP vesicles after LIC1 RNAi treatment. Insets show enlargements of boxed areas. Scale bars, 5 μm.

reflect multiple dynein recruitment or regulatory mechanisms. Further work will be needed to explore the relative roles of these factors in detail.

MATERIALS AND METHODS
cDNAs and antibodies
Cloning of myc-tagged p50 was described previously (Echeverri et al., 1996). Cloning of rat LIC1 and LIC2 into pCMV-HA-LIC1 and pCMV-Flag-LIC2 and the generation of the pan-LIC and anti-LIC2 antibodies were also described previously (Tynan et al., 2000b). The LIC constructs were used for site-directed mutagenesis (QuikChange II, Agilent Stratagene, Cedar Creek, TX) to make them resistant to LIC siRNAs. Primer sequences were GCCGAGCTCGA-CAGAAT**A**AC**G**CG**C**AAACCTGCTTCTG and CGTTCAGGAA-GAACTGGA**CC**G**T**ATGACTCGAAAACCAGACTCC for LIC1 and LIC2, respectively, introducing three silent point mutations (bold letters). With AvesLabs, antibody to rat LIC1 was raised in chicken against the C-terminal 18–amino acid sequence of rat LIC1 (PAS-VSPTTPPSPTEGEAS) and affinity purified. Polyclonal antibodies to dynein HC and ZW10 were described previously (Starr et al., 1998; Mikami et al., 2002), and the monoclonal antibody (mAb) to dynein IC was purchased from Chemicon International (Billerica, MA). The mAb to p150[Glued] was purchased from Signal Transduction Laboratories. The polyclonal anti-myc antibody used in this study

was described previously (Gee et al., 1997). The monoclonal anti-myc antibody 9E10 was also described elsewhere (Evan et al., 1985). The mAbs against the HA and Flag tags were purchased from Covance (Princeton, NJ) and Sigma-Aldrich (St. Louis, MO), respectively. The mAbs EEA1 and GM130 were purchased from BD Biosciences (Franklin Lakes, NJ), anti-LAMP1 was obtained from Genetex (Irvine, CA), and Abcam (Cambridge, MA), and anti–α-tubulin was purchased from Sigma-Aldrich. pCMV-EGFP–tagged EGFR was a gift from the laboratory of Sanford Simon (Rockefeller University, New York, NY), pCMV-GFP-RILP and ΔN-RILP were gifts from Sergio Grinstein (University of Toronto at Scarborough, Toronto, Canada), and pCMV-GFP-Rab7 and pCMV-GFP-CD63 were gifts from Cecilia Bucci (Universita del Salento, Lecce, Italy).

Cell culture and RNAi
Rat2 and HeLa cells were grown in DMEM with 10% fetal calf serum. To depolymerize microtubules, cells were treated with 10 μM nocodazole for 2 h. Nocodazole was then washed out with phosphate-buffered saline (PBS) before fixation and immunostaining. siRNA were prepared and according to the specifications of the manufacturer (Dharma-con RNA Technologies, Lafayette, CO) and transfected with Effectene (Qiagen, Valencia, CA) at a final concentration of 10 μM. The RNA sequences used for LIC1 siRNA were GUUGAUUAGAGACUUCCAATT (LIC1a) and CGACAGAAUCACACG-GAAAUU (LIC1b). For LIC2 siRNA, the sequences were GGAUAGAAUGACUCGAAAAUU (LIC2a) and UG-GAGAAGGAGCACGAUUAUU (LIC2b; Shanghai GenePharma, Shanghai, China). For a scrambled negative control, the sequence used was AUUGUAUGCGAUCGCAGACUU. The target sequence used for siRNA against ZW10 was AAGGGUGAGGUGUG-CAAUAG. The efficiencies of the siRNA oligonucleotides were tested against both endogenous LIC1 and LIC2 and recombinant HA-LIC1 and Flag-LIC2 in Rat2 cell lysates via SDS–PAGE and Western blotting with antibodies against HA and Flag tags as well as antibodies against LIC1 and LIC2 specifically. For LIC siRNA rescue experiments, cells were transfected with siRNA-resistant constructs 24 h after siRNA transfection.

Immunofluorescence microscopy
Cells were grown on coverslips and before staining, rinsed in PBS, and fixed at room temperature for 15 min in 4% paraformaldehyde, followed by 0.5% saponin for 5 min for endosome and lysosome staining or cold MeOH for Golgi staining. Cells were blocked in 1% bovine serum albumin (BSA) in PBS for 30 min at room temperature before primary antibody incubation in 0.1% BSA in PBS overnight at 4°C. Coverslips were then washed for 30 min in PBS, incubated with fluorescently conjugated secondary antibodies for 1 h at 37°C, washed for another 30 min in PBS, and stained with 4′,6-diamino-2-phenylindole (DAPI) before mounting on glass slides. Lysosomes were labeled for live cell imaging with the fluorescent lysosomal dye
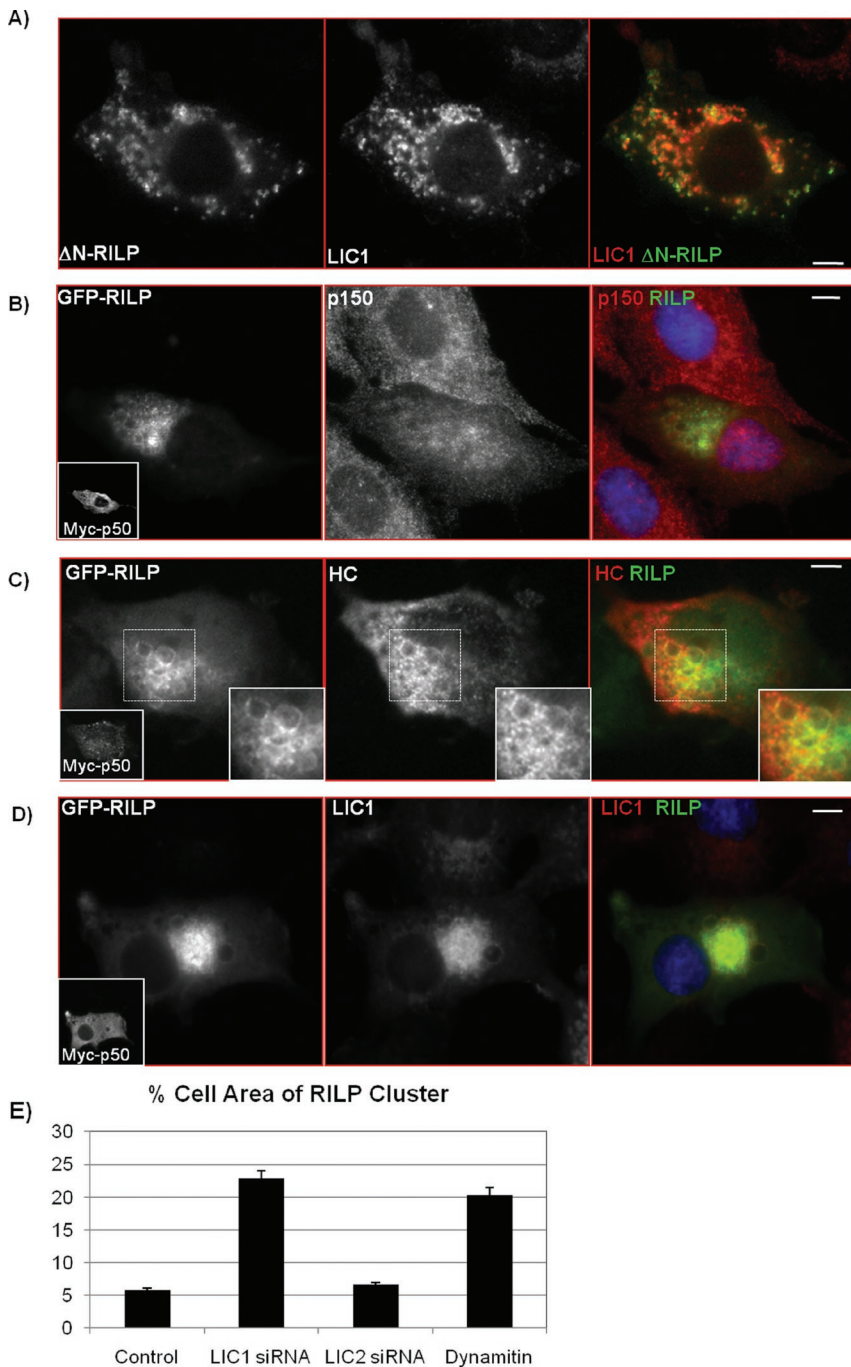
FIGURE 8: Dynein remains with lysosomes dispersed by ΔN-RILP and localizes to RILP clusters after dynamitin (p50) overexpression despite displacement of dynactin. (A) Immunocytochemistry of Rat2 cells overexpressing a GFP-tagged C-terminal fragment of RILP, GFP–ΔN-RILP (green), and stained for LIC1 (red). (B–D) Despite displacing dynactin from enlarged RILP vesicles, dynamitin (p50) overexpression does not displace HC or LIC1. Rat2 cells cotransfected with myc-p50 and GFP-RILP were immunostained with anti-p150 and anti-myc antibodies (B), anti-HC and anti-myc antibodies (C), or anti-LIC1 and anti-myc antibodies (D). Myc-p50–transfected cells shown in insets. All merges show p150, HC, and LIC1 in red and GFP-RILP in green. (C) Insets are zoomed images of areas outlined in hashed boxes (bottom). Here, clear and distinct HC puncta are seen overlapping with enlarged RILP vesicles after p50 overexpression (C), despite loss of p150[Glued] (B). (D) LIC1 is also not displaced from RILP-positive lysosomes in cells coexpressing myc-p50 and GFP-RILP. Scale bars, 5 μm. (E) Effects of LIC siRNA treatment and dynamitin overexpression on RILP clusters. To quantify the percent area of the cell occupied by RILP-clustered lysosomes, the total area of RILP-positive fluorescence is compared with the total area of the cell and is represented as percent area of the cell. Averages are shown where at least 30 cells were counted per condition from three experiments each.

LysoTracker-Red. Briefly, cells were treated with LysoTracker at a concentration of 0.2 μM for 1 h. Excess LysoTracker was then washed out and replaced with 10% DMEM before imaging.

Images were obtained using an Olympus IX-71 microscope with a DSU spinning disk with a Hamamatsu EM-CCD camera and MetaMorph Software (Universal Imaging Corporation, Buckinghamshire, UK). Z-series stacks were acquired with 0.2-μm steps. Laser confocal microscopy was also performed with a Nikon Diaphot 200 microscope coupled to a system equipped with a Kr/Ar laser (MRC1000; Bio-Rad Laboratories, Hercules, CA). All images were visualized using a 63× oil-immersion objective lens, quantification of colocalization was performed using MetaMorph Software, and the occupied cell area data were analyzed and quantified using ImageJ.

Late endosome and lysosome purification

The late endosomal and lysosomal fractions from Rat2 cells were prepared as described (Aniento et al., 1993). Briefly, cells were first harvested and homogenized in homogenization buffer (8% sucrose, 3 mM imidazole, pH 7.4), from which a postnuclear supernatant (PNS) was prepared and adjusted to 40.6% sucrose. The PNS was then loaded into the bottom of an SW50.1 tube and overlaid sequentially with 35%, 27% sucrose solutions in 3 mM imidazole, pH 7.4, and homogenization buffer. Gradients were centrifuged for 1 h at $100,000 \times g$ followed by collection of fractions at the interfaces of 40–35%, 35–27%, and 27–8% sucrose.

EGFR degradation assay

Rat2 cells grown on coverslips and treated with either scrambled RNAi or RNAi against LIC1 were pretreated with 10 μg/ml cycloheximide for 1 h before stimulated with 50 ng/ml EGF (Sigma-Aldrich) for 15, 30, 60, or 120 min. Cells were then fixed and stained as mentioned above before imaging. The intensities of the EGFR staining for each condition were quantified using MetaMorph software and plotted as a percentage of the respective intensities after 15 min of EGF stimulation.

Sucrose density gradient centrifugation and LIC incorporation assays

For each gradient, two 10-cm dishes each of Rat2 cells treated with either scrambled or LIC1 RNAi were trypsinized and lysed in RIPA buffer and centrifuged for 30 min at 65,000 rpm on an MLA-80 rotor. The supernatants were then loaded on top of a 5-ml 20–5% sucrose step gradient consisting of four layers of 20%, 15%, 10%, and 5% sucrose from the bottom of the gradient to the top, respectively. The gradients were then centrifuged on a TLS55 rotor for 3 h at 54,000 rpm, and fractions were collected and precipitated with trichloroacetic acid to concentrate them for immunoblotting. All centrifugation steps were performed at 4°C.
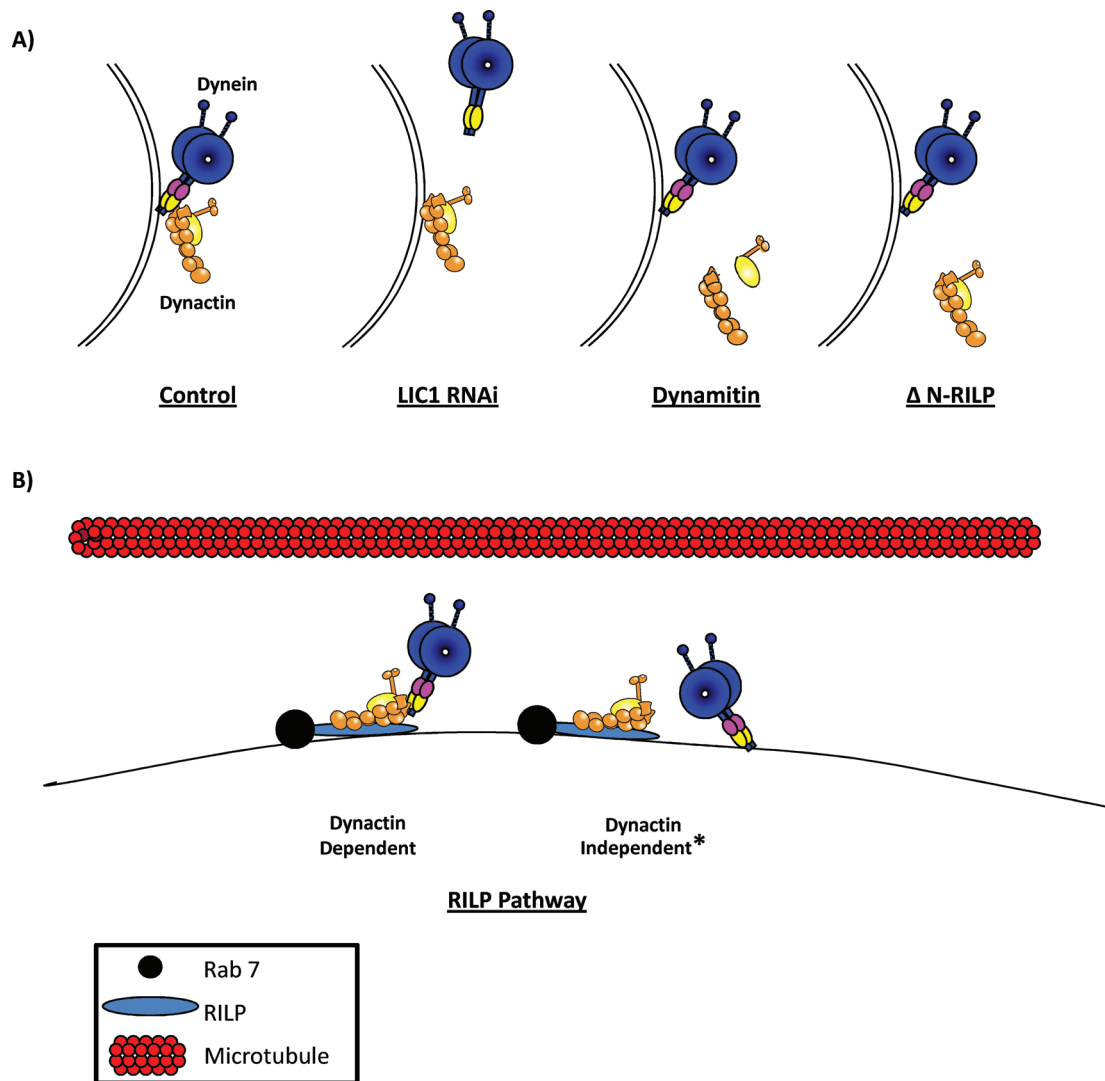
FIGURE 9: The effects of LIC RNAi, dynamitin overexpression, and ΔN-RILP on the recruitment of dynein and dynactin to late endosomes and lysosomes and parallel models for dynein recruitment to late endosomes and lysosomes. (A) LIC1 RNAi displaces dynein independently of dynactin while overexpression of dynamitin, which dissociates the dynein–dynactin interaction, or ΔN-RILP, which lacks full-length RILP's dynactin interaction region, has no effect on dynein recruitment despite displacement of dynactin. Subunits depicted on dynein motor are the LICs (pink) and the ICs (yellow). (B) Models for possible means of recruiting dynein to late endocytic vesicles: dynactin dependent, through dynactin's interaction with RILP (blue, Rab7 also shown in black and microtubules in red), or dynactin independent. *Dynactin-independent recruitment can happen through either an independent interaction with RILP or recruitment to the vesicular surface separately and independently of both dynactin and RILP.

Recombinant LIC incorporation into the dynein complex was tested by incubating lysate of untransfected Rat2 cells and cells overexpressing either HA-LIC1 or Flag-LIC2 with protein A-Sepharose and an anti-HA or anti-Flag mAb for 1.5 h at 4°C. After centrifugation and extensive washing, supernatants and pellets were subjected to SDS–PAGE and Western blotting.

REFERENCES

Aniento F, Emans N, Griffiths G, Gruenberg J (1993). Cytoplasmic dynein-dependent vesicular transport from early to late endosomes. J Cell Biol 123, 1373–1387.

Bananis E, Nath S, Gordon K, Satir P, Stockert RJ, Murray JW, Wolkoff AW (2004). Microtubule-dependent movement of late endocytic vesicles in vitro: requirements for dynein and kinesin. Mol Biol Cell 15, 3688–3697.

Burkhardt JK (1998). The role of microtubule-based motor proteins in maintaining the structure and function of the Golgi complex. Biochim Biophys Acta 1404, 113–126.

Burkhardt JK, Echeverri CJ, Nilsson T, Vallee RB (1997). Overexpression of the dynamitin (p50) subunit of the dynactin complex disrupts dynein-dependent maintenance of membrane organelle distribution. J Cell Biol 139, 469–484.

Caviston JP, Ross JL, Antony SM, Tokito M, Holzbaur EL (2007). Huntingtin facilitates dynein/dynactin-mediated vesicle transport. Proc Natl Acad Sci USA 104, 10045–10050.

Deacon SW, Serpinskaya AS, Vaughan PS, Lopez Fanarraga M, Vernos I, Vaughan KT, Gelfand VI (2003). Dynactin is required for bidirectional organelle transport. J Cell Biol 160, 297–301.

Dell KR, Turck CW, Vale RD (2000). Mitotic phosphorylation of the dynein light intermediate chain is mediated by cdc2 kinase. Traffic 1, 38–44.

Driskell OJ, Mironov A, Allan VJ, Woodman PG (2007). Dynein is required for receptor sorting and the morphogenesis of early endosomes. Nat Cell Biol 9, 113–120.

Dujardin DL, Barnhart LE, Stehman SA, Gomes ER, Gundersen GG, Vallee RB (2003). A role for cytoplasmic dynein and LIS1 in directed cell movement. J Cell Biol 163, 1205–1211.

Echeverri CJ, Paschal BM, Vaughan KT, Vallee RB (1996). Molecular characterization of the 50-kD subunit of dynactin reveals function for the complex in chromosome alignment and spindle organization during mitosis. J Cell Biol 132, 617–633.

Evan GI, Lewis GK, Ramsay G, Bishop JM (1985). Isolation of monoclonal antibodies specific for human c-myc proto-oncogene product. Mol Cell Biol 5, 3610–3616.

Gee MA, Heuser JE, Vallee RB (1997). An extended microtubule-binding structure within the dynein motor domain. Nature 390, 636–639.

Grissom PM, Vaisberg EA, McIntosh JR (2002). Identification of a novel light intermediate chain (D2LIC) for mammalian cytoplasmic dynein 2. Mol Biol Cell 13, 817–829.

Ha J, Lo KW, Myers KR, Carr TM, Humsi MK, Rasoul BA, Segal RA, Pfister KK (2008). A neuron-specific cytoplasmic dynein isoform preferentially transports TrkB signaling endosomes. J Cell Biol 181, 1027–1039.

Habermann A, Schroer TA, Griffiths G, Burkhardt JK (2001). Immunolocalization of cytoplasmic dynein and dynactin subunits in cultured macrophages: enrichment on early endocytic organelles. J Cell Sci 114, 229–240.

Haghnia M, Cavalli V, Shah SB, Schimmelpfeng K, Brusch R, Yang G, Herrera C, Pilling A, Goldstein LS (2007). Dynactin is required for coordinated bidirectional motility, but not for dynein membrane attachment. Mol Biol Cell 18, 2081–2089.

Harada A, Takei Y, Kanai Y, Tanaka Y, Nonaka S, Hirokawa N (1998). Golgi vesiculation and lysosome dispersion in cells lacking cytoplasmic dynein. J Cell Biol 141, 51–59.

Holleran EA, Ligon LA, Tokito M, Stankewich MC, Morrow JS, Holzbaur EL (2001). βIII Spectrin binds to the Arp1 subunit of dynactin. J Biol Chem 276, 36598–36605.

Jordens I, Fernandez-Borja M, Marsman M, Dusseljee S, Janssen L, Calafat J, Janssen H, Wubbolts R, Neefjes J (2001). The Rab7 effector protein RILP controls lysosomal transport by inducing the recruitment of dynein-dynactin motors. Curr Biol 11, 1680–1685.

Karki S, Holzbaur EL (1995). Affinity chromatography demonstrates a direct binding between cytoplasmic dynein and the dynactin complex. J Biol Chem 270, 28806–28811.

Karki S, Ligon LA, DeSantis J, Tokito M, Holzbaur EL (2002). PLAC-24 is a cytoplasmic dynein-binding protein that is recruited to sites of cell-cell contact. Mol Biol Cell 13, 1722–1734.

King SJ, Schroer TA (2000). Dynactin increases the processivity of the cytoplasmic dynein motor. Nat Cell Biol 2, 20–24.

Koushika SP, Schaefer AM, Vincent R, Willis JH, Bowerman B, Nonet ML (2004). Mutations in Caenorhabditis elegans cytoplasmic dynein components reveal specificity of neuronal retrograde cargo. J Neurosci 24, 3907–3916.

Lippincott-Schwartz J (1998). Cytoskeletal proteins and Golgi dynamics. Curr Opin Cell Biol 10, 52–59.

Lo KW, Kogoy JM, Pfister KK (2007). The DYNLT3 light chain directly links cytoplasmic dynein to a spindle checkpoint protein, Bub3. J Biol Chem 282, 11205–11212.

Malone CJ, Misner L, Le Bot N, Tsai MC, Campbell JM, Ahringer J, White JG (2003). The C. elegans hook protein, ZYG-12, mediates the essential attachment between the centrosome and nucleus. Cell 115, 825–836.

Matanis et al. T (2002). Bicaudal-D regulates COPI-independent Golgi-ER transport by recruiting the dynein-dynactin motor complex. Nat Cell Biol 4, 986–992.

Mikami A, Tynan SH, Hama T, Luby-Phelps K, Saito T, Crandall JE, Besharse JC, Vallee RB (2002). Molecular structure of cytoplasmic dynein 2 and its distribution in neuronal and ciliated cells. J Cell Sci 115, 4801–4808.

Palmer KJ, Hughes H, Stephens DJ (2009). Specificity of cytoplasmic dynein subunits in discrete membrane-trafficking steps. Mol Biol Cell 20, 2885–2899.

Perrone CA, Tritschler D, Taulman P, Bower R, Yoder BK, Porter ME (2003). A novel dynein light intermediate chain colocalizes with the retrograde motor for intraflagellar transport at sites of axoneme assembly in Chlamydomonas and mammalian cells. Mol Biol Cell 14, 2041–2056.

Presley JF, Cole NB, Schroer TA, Hirschberg K, Zaal KJ, Lippincott-Schwartz J (1997). ER-to-Golgi transport visualized in living cells. Nature 389, 81–85.

Progida C, Malerod L, Stuffers S, Brech A, Bucci C, Stenmark H (2007). RILP is required for the proper morphology and function of late endosomes. J Cell Sci 120, 3729–3737.

Progida C, Spinosa MR, De Luca A, Bucci C (2006). RILP interacts with the VPS22 component of the ESCRT-II complex. Biochem Biophys Res Commun 347, 1074–1079.

Purohit A, Tynan SH, Vallee R, Doxsey SJ (1999). Direct interaction of pericentrin with cytoplasmic dynein light intermediate chain contributes to mitotic spindle organization. J Cell Biol 147, 481–492.

Reilein AR, Serpinskaya AS, Karcher RL, Dujardin DL, Vallee RB, Gelfand VI (2003). Differential regulation of dynein-driven melanosome movement. Biochem Biophys Res Commun 309, 652–658.

Roghi C, Allan VJ (1999). Dynamic association of cytoplasmic dynein heavy chain 1a with the Golgi apparatus and intermediate compartment. J Cell Sci 112, 4673–4685.

Schmoranzer J, Fawcett JP, Segura M, Tan S, Vallee RB, Pawson T, Gundersen GG (2009). Par3 and dynein associate to regulate local microtubule dynamics and centrosome orientation during migration. Curr Biol 19, 1065–1074.

Short B, Preisinger C, Schaletzky J, Kopajtich R, Barr FA (2002). The Rab6 GTPase regulates recruitment of the dynactin complex to Golgi membranes. Curr Biol 12, 1792–1795.

Sivaram MV, Wadzinski TL, Redick SD, Manna T, Doxsey SJ (2009). Dynein light intermediate chain 1 is required for progress through the spindle assembly checkpoint. EMBO J 28, 902–914.

Starr DA, Williams BC, Hays TS, Goldberg ML (1998). ZW10 helps recruit dynactin and dynein to the kinetochore. J Cell Biol 142, 763–774.

Tai AW, Chuang JZ, Bode C, Wolfrum U, Sung CH (1999). Rhodopsin's carboxy-terminal cytoplasmic tail acts as a membrane receptor for cytoplasmic dynein by binding to the dynein light chain Tctex-1. Cell 97, 877–887.

Tai AW, Chuang JZ, Sung CH (2001). Cytoplasmic dynein regulation by subunit heterogeneity and its role in apical transport. J Cell Biol 153, 1499–1509.

Tynan SH, Gee MA, Vallee RB (2000a). Distinct but overlapping sites within the cytoplasmic dynein heavy chain for dimerization and for intermediate chain and light intermediate chain binding. J Biol Chem 275, 32769–32774.

Tynan SH, Purohit A, Doxsey SJ, Vallee RB (2000b). Light intermediate chain 1 defines a functional subfraction of cytoplasmic dynein which binds to pericentrin. J Biol Chem 275, 32763–32768.

Varma D, Dujardin DL, Stehman SA, Vallee RB (2006). Role of the kinetochore/cell cycle checkpoint protein ZW10 in interphase cytoplasmic dynein function. J Cell Biol 172, 655–662.

Vaughan KT, Vallee RB (1995). Cytoplasmic dynein binds dynactin through a direct interaction between the intermediate chains and p150Glued. J Cell Biol 131, 1507–1516.

Wang T, Hong W (2006). RILP interacts with VPS22 and VPS36 of ESCRT-II and regulates their membrane recruitment. Biochem Biophys Res Commun 350, 413–423.

Williams JC, Roulhac PL, Roy AG, Vallee RB, Fitzgerald MC, Hendrickson WA (2007). Structural and thermodynamic characterization of a cytoplasmic dynein light chain-intermediate chain complex. Proc Natl Acad Sci USA 104, 10028–10033.

Wu M, Wang T, Loh E, Hong W, Song H (2005). Structural basis for recruitment of RILP by small GTPase Rab7. EMBO J 24, 1491–1501.

Yeh TY, Peretti D, Chuang JZ, Rodriguez-Boulan E, Sung CH (2006). Regulatory dissociation of Tctex-1 light chain from dynein complex is essential for the apical delivery of rhodopsin. Traffic 7, 1495–1502.

Yoder JH, Han M (2001). Cytoplasmic dynein light intermediate chain is required for discrete aspects of mitosis in Caenorhabditis elegans. Mol Biol Cell 12, 2921–2933.

Young A, Dictenberg JB, Purohit A, Tuft R, Doxsey SJ (2000). Cytoplasmic dynein-mediated assembly of pericentrin and gamma tubulin onto centrosomes. Mol Biol Cell 11, 2047–2056.